Article

Cell Reports

The Transcription Factor Tcf1 Contributes to Normal NK Cell Development and Function by Limiting the Expression of Granzymes

Graphical Abstract

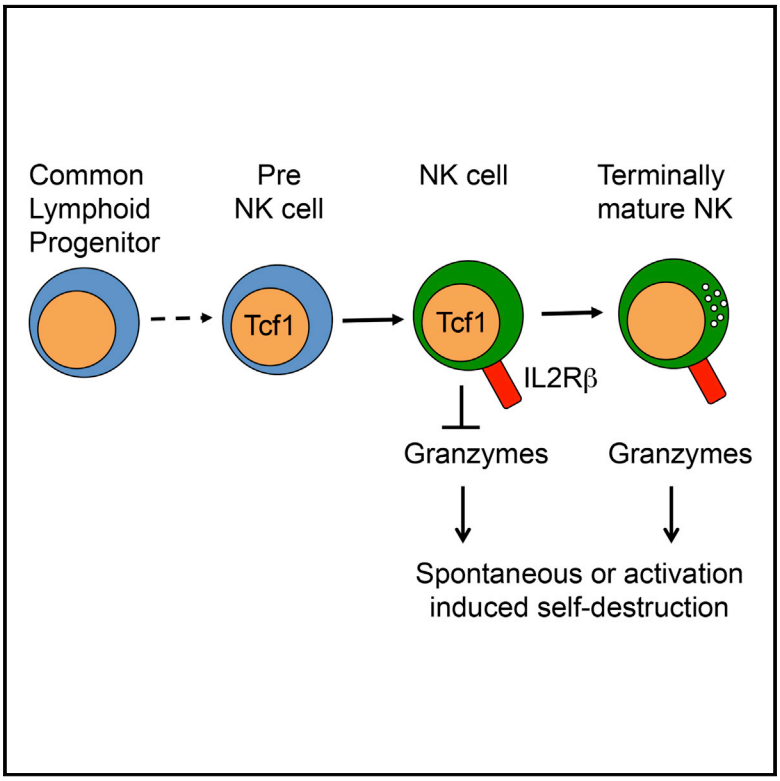

Authors

Beena Jeevan-Raj, Jasmine Gehrig, Mélanie Charmoy, ..., Paolo Angelino, Mauro Delorenzi, Werner Held

Correspondence

werner.held@unil.ch

In Brief

The transcription factor Tcf1 is essential for NK cell development, but its role has not been clarified. Jeevan-Raj et al. identify a stage-specific role for Tcf1 in ensuring the survival of NK-committed cells. Tcf1 limited the expression of granzymes, thereby preventing granzyme-mediated NK cell self-destruction.

Highlights

- Tcf1 ensures NK cell survival during maturation and upon activation
- Tcf1-deficient NK cells overexpress granzymes
- Granzyme overexpression results in NK cell self-destruction
- Tcf1 binding to an upstream regulatory element limits granzyme B expression

Accession Numbers

GSE92711

Jeevan-Raj et al., 2017, Cell Reports *20*, 613–626
July 18, 2017
http://dx.doi.org/10.1016/j.celrep.2017.06.071

Cell Reports
Article

The Transcription Factor Tcf1 Contributes to Normal NK Cell Development and Function by Limiting the Expression of Granzymes

Beena Jeevan-Raj,[1,3] Jasmine Gehrig,[1,4] Mélanie Charmoy,[1] Vijaykumar Chennupati,[1] Camille Grandclément,[1,5] Paolo Angelino,[2] Mauro Delorenzi,[2] and Werner Held[1,6,*]
[1]Ludwig Cancer Research Center, Department of Fundamental Oncology, University of Lausanne, 1066 Epalinges, Switzerland
[2]SIB Swiss Institute of Bioinformatics, Bioinformatics Core Facility, 1015 Lausanne, Switzerland
[3]Present address: Department of Biomedicine, University of Basel, 4058 Basel, Switzerland
[4]Present address: AstraZeneca, 6031 Zug, Switzerland
[5]Present address: Transcure Bioservices, 74160 Archamps, France
[6]Lead Contact
*Correspondence: werner.held@unil.ch
http://dx.doi.org/10.1016/j.celrep.2017.06.071

SUMMARY

The transcription factor Tcf1 is essential for the development of natural killer (NK) cells. However, its precise role has not been clarified. Our combined analysis of Tcf1-deficient and transgenic mice indicated that Tcf1 guides NK cells through three stages of development. Tcf1 expression directed bone marrow progenitors toward the NK cell lineage and ensured the survival of NK-committed cells, and its downregulation was needed for terminal maturation. Impaired survival of NK-committed cells was due to excessive expression of granzyme B (GzmB) and other granzyme family members, which induced NK cell self-destruction during maturation and following activation with cytokines or target cells. Mechanistically, Tcf1 binding reduced the activity of a *Gzmb*-associated regulatory element, and this accounted for the reduced *Gzmb* expression in Tcf1-expressing NK cells. These data identify an unexpected requirement to limit the expression of cytotoxic effector molecules for the normal expansion and function of NK cells.

INTRODUCTION

Natural killer (NK) cells represent the innate counterpart of cytotoxic $CD8^+$ T cells and play important roles in the clearance of not only certain pathogens but also pathogen-infected and transformed host cells. While $CD8^+$ T cells use somatically rearranged T cell receptors (TCRs) to detect antigens on host cells, NK cells utilize a set of germline-encoded activation and inhibition receptors to determine whether host cells express specific self-ligands at normal levels. Both effector cell types respond to aberrant host cells by the production of cytokines, including interferon-γ (IFN-γ), and by the directed release of cytolytic granules containing perforin and multiple distinct granzymes, which trigger a suicide program in target cells.

While all lymphocytes can be derived from bone marrow (BM) resident common lymphoid progenitors (CLPs), lymphocytes lacking antigen receptors (i.e., innate lymphoid cells [ILCs] and NK cells) can be derived from a shared downstream early innate lymphoid progenitor (EILP) (Yang et al., 2015). Subsequently, NK cells arise via the pre-NK ($Lin^-CD127^+CD135^-CD122^-$) and rNK ($Lin^-CD127^+CD135^-CD122^+$) stages (Carotta et al., 2011; Fathman et al., 2011). Even though pre-NK cells efficiently give rise to NK cells, it is not clear whether they have lost ILC potential. Based on the upregulation of interleukin-2/15Rβ (IL-2/15Rβ) (CD122), rNK cells may be considered the earliest NK-cell-lineage-committed progenitor. Indeed, IL-15 receptor signaling is a critical rate-limiting step for NK cell development, expansion, and survival (Vosshenrich et al., 2005). Further development is characterized by the acquisition of germline-encoded NK cell receptors and an expansion phase, which yields a pool of mature ($CD122^+DX5^+NK1.1^+$) BM NK cells (mNK). An additional hallmark of NK cell development is the acquisition of an effector cell program in their tissue of origin. BM NK cells constitutively express considerable levels of perforin, granzyme B (GzmB), and IFN-γ mRNAs that are, however, not efficiently translated into protein (Fehniger et al., 2007; Stetson et al., 2003). Further NK cell maturation can be followed based on the transient upregulation of CD27 followed by the upregulation CD11b and KLRG1. During this maturation, NK cells progressively lose homeostatic expansion capacity, gain cytolytic potential (Chiossone et al., 2009), and become prone to apoptosis (Robbins et al., 2004).

Several transcription factors impact specific stages of NK cell development and maturation. For example, Nfil3 (E4BP4) commits progenitors to the NK cell lineage (Male et al., 2014), and Eomes, together with T-bet (*Tbx21*), is essential for the further development of NK-committed progenitors (Gascoyne et al., 2009; Gordon et al., 2012). The latter and additional transcription factors (e.g., Id2) act at least in part by improving the responsiveness of immature NK cells to IL-15 (Delconte et al., 2016; Intlekofer et al., 2005). On the other hand, multiple aspects of the NK cell developmental program including for example the acquisition of NK cell receptors, the establishment of the effector program, and relevant control mechanisms, remain poorly understood.

The transcription factor Tcf1 (encoded by the *Tcf7* gene) was initially found to be required for the acquisition of certain Ly49 family NK cell receptors as well as for NK cell development (Held et al., 1999). More recently it was shown that pre-NK cells as well as NK-lineage-committed rNK and mNK cells are severely reduced in the absence of Tcf1 (Yang et al., 2015). Tcf1 binds DNA in a sequence-specific fashion and can directly repress target genes by exerting histone deacetylase (HDAC) activity or via association with Groucho/TLE co-repressors (Roose et al., 1998; Xing et al., 2016). In addition, Tcf1 can mediate the nuclear response to extracellular Wnt proteins by binding β-catenin and/or γ-catenin (Jeannet et al., 2008; Molenaar et al., 1996). The precise role of Tcf1 in NK cell development and essential targets have not been identified.

Here, we find that Tcf1 expression directs lymphoid progenitors toward the NK cell lineage and ensures the survival of NK-lineage-committed cells, and we also find that Tcf1 downregulation is required for terminal NK cell maturation. Tcf1 ensured NK cell survival during maturation and following activation by preventing excessive granzyme expression, which induced NK cell self-destruction. Tcf1 reduced the activity a regulatory element in the vicinity of the *Gzmb* locus, and this accounted for reduced GzmB expression. Limiting the expression of granzymes thus plays an unexpected and essential role for NK cell development.

RESULTS

Tcf1 Expression Is Upregulated Prior to NK Cell Commitment and Ceases during Terminal Maturation

To define the role of the transcription factor Tcf1 for NK cell development, we analyzed Tcf1 expression in a series of BM progenitors. Using a Tcf1 reporter mouse strain (Utzschneider et al., 2016) in which GFP expression is controlled by the *Tcf7* locus (*Tcf7*-GFP) (Figures S1A–S1C), we confirmed lack of *Tcf7*-GFP expression in CLP (defined as detailed in Experimental Procedures) and expression in downstream Lin^-CD127^- $Thy1.2^-$ BM cells (Figures 1A and 1B) (Yang et al., 2015). *Tcf7*-GFP was also homogenously expressed by pre-NK and rNK cells (Figure 1A) and by subsets of immature NK (iNK) cells, mNK cells, and splenic NK cells (Figures 1C and 1D). Differentiating splenic NK cells according to their maturational states (Chiossone et al., 2009) revealed that *Tcf7*-GFP expression was high in immature ($CD27^+CD11b^-$) NK cells, reduced in intermediate ($CD27^+CD11b^+$) NK cells, and essentially absent in terminally mature ($CD27^-CD11b^+$) NK cells (Figure 1D), in agreement with Tcf1 protein expression (Figure 1E). The *Tcf7*-GFP reporter and intracellular staining detect Tcf1 isoforms that contain an extended N terminus. Western blots using an antibody specific for a central portion of Tcf1 showed that splenic NK cells almost exclusively expressed the p45 Tcf1 isoform (Figure S1D), which contains DNA-binding, repressor, and N-terminal catenin-binding domains (schematically depicted in Figure S1A). Thus Tcf1 expression is induced prior to the commitment of BM progenitors to the NK cell lineage and expression ceases upon terminal NK cell maturation.

Tcf1 Expression Is Essential for NK Cell Development, and Its Downregulation Is Required for Terminal Maturation

We next addressed the Tcf1 dependence of NK cell developmental. In the absence of Tcf1, CLPs were present normally, but EILPs were significantly reduced (Figures 2A–2C). Further, pre-NK, rNK, and mNK cell populations were reduced 3- to >10-fold in the absence of Tcf1 (Figures 2B–2E), in agreement with previous findings (Yang et al., 2015). To address whether subdomains of Tcf1 play selective roles in NK cell development, we analyzed $Tcf7^{-/-}$ mice expressing either a full-length (p45) or N-terminally truncated (p33) Tcf1 transgene (Tg). The two Tg's share known Tcf1 functions, except that p33 cannot bind β- and γ-catenin (Figure S1A). The NK cell developmental defect of $Tcf7^{-/-}$ mice was rescued by the p45 Tg, but not by the p33 Tg (Figures 2B–2E). Detailed analysis of BM progenitors revealed that the p45 Tg expanded CLPs and restored the pre-NK, rNK, and mNK compartments (Figures 2B–2E). Unexpectedly, p33 expression similarly expanded CLPs and restored pre-NK cells but failed to rescue rNK and mNK cells (Figures 2B–2E). Since homeostatic expansion of residual progenitors or NK cells may mask developmental effects, we further analyzed competitive irradiation BM chimeras. These analyses confirmed that absence of Tcf1 reduced the pre-NK cell population and profoundly impaired rNK and mNK cell development. Further the p33 Tg restored pre-NK cells but did not rescue (or only marginally rescued) rNK and mNK cells (Figure S2A). Mixed BM chimeras further revealed that $Tcf7^{-/-}$ BM contributed inefficiently to the splenic NK cell compartment and that the p45 Tg, but not the p33 Tg, rescued splenic NK cells (Figure S2B). Conversely, NK cell development was normal when $Tcf7^{+/+}$ BM progenitors matured in $Tcf7^{-/-}$ hosts (data not shown). These data indicated that enforced Tcf1 expression restored NK cell development whereby the catenin-binding domain in Tcf1 (present in p45) was not essential to direct BM progenitors toward the NK cell lineage but was needed to expand NK-committed cells.

Despite impaired NK cell development, we noted only minor differences in the expression of activating NK cell receptors (including NK1.1, NKp46, NKG2D, CD16, Ly49H [except for a reduced presence of $Ly49D^+$ NK cells], or SLAM family receptors [SLAM, 2B4, CD84, Ly-9, Ly-108, and CRACC]) in the absence of Tcf1 (data not shown). On the other hand, the expression of several inhibitory receptors specific for major histocompatibility complex (MHC) class I molecules, particularly Ly49A, was significantly altered (data not shown), as reported before (Held et al., 1999). In addition, terminally mature BM and spleen NK cells ($CD27^-CD11b^+$ or $KLRG1^+$) were significantly more abundant in $Tcf7^{-/-}$ mice (Figures 3 and S3A). A corresponding albeit weaker effect was observed in mixed BM chimeras (Figure S3B), indicating that the absence of $Tcf7^{-/-}$ promoted terminal maturation. Enforced Tcf1 (p45) expression resulted in efficient CD27 upregulation but yielded few terminally mature NK cells ($CD27^-CD11b^+$ or $KLRG1^+$) (Figures 3 and S3A). These findings, together with the lack of Tcf1 in terminally mature wild-type NK cells (Figures 1D and 1E), suggested that Tcf1 downregulation was required for terminal differentiation. Thus, Tcf1 expression promoted NK cell development, while its downregulation allowed terminal maturation.

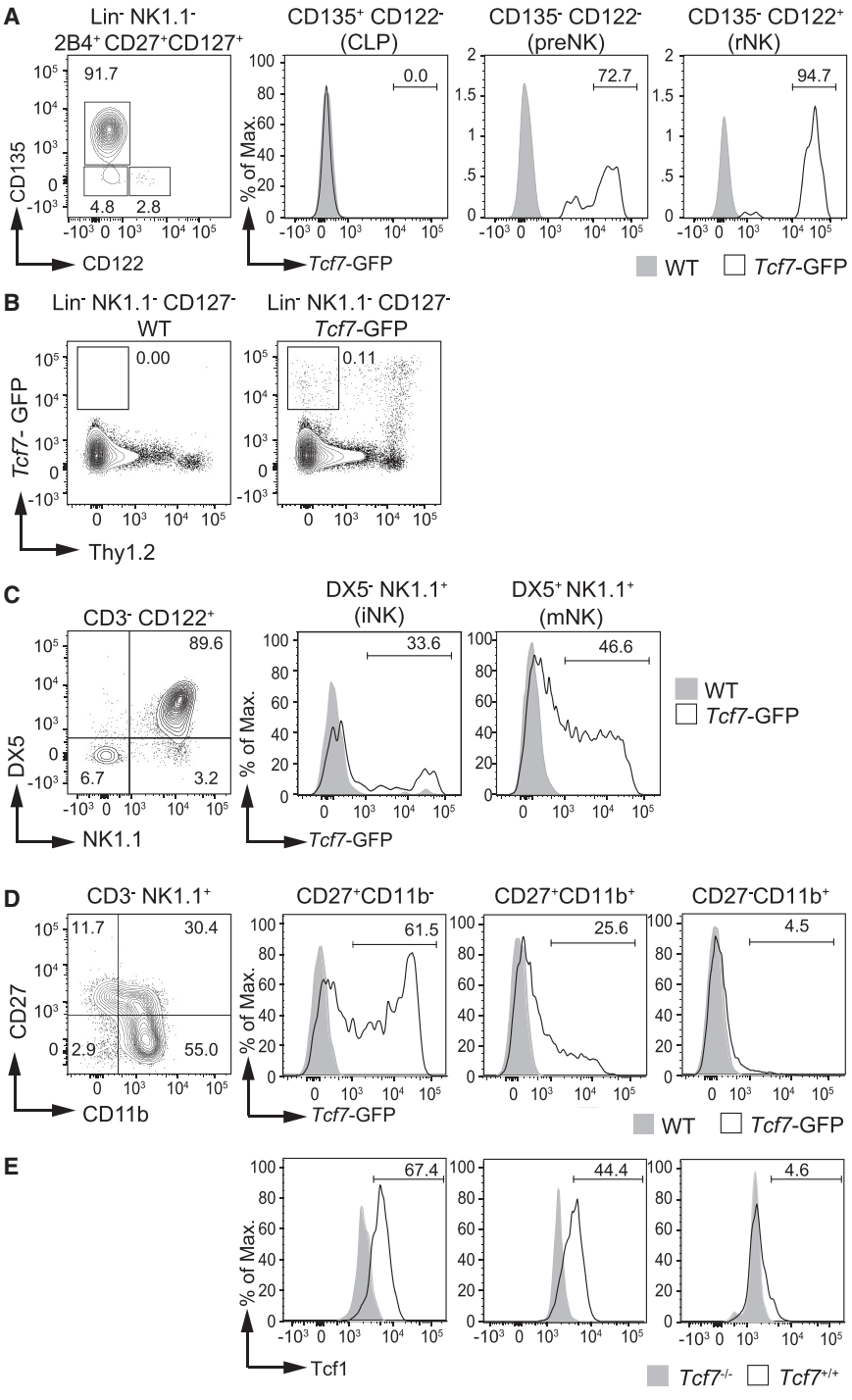

Figure 1. Tcf1 Expression during NK Cell Development and Maturation

(A) Lin$^-$NK1.1$^-$2B4$^+$CD27$^+$CD127$^+$ bone marrow (BM) cells were subdivided into common lymphoid progenitors (CLPs) (CD135$^+$CD122$^-$), pre-NK cells (CD135$^-$CD122$^-$), and rNK cells (CD135$^-$CD122$^+$) and analyzed for Tcf1 expression using a *Tcf7*-GFP reporter mouse strain. Histogram overlays show *Tcf7*-GFP expression (open histograms) as compared to cells from wild-type (WT) non-reporter mice (gray fill). Numbers indicate the percentage of cells in the respective gate.

(B) Lin$^-$NK1.1$^-$CD127$^-$ BM cells were analyzed for Thy1.2 versus *Tcf7*-GFP expression, which identifies a population of Thy1$^-$*Tcf7*-GFP$^+$ cells, which represent early innate lymphoid progenitors (EILPs).

(C) CD3$^-$CD122$^+$ BM NK cells were subdivided into iNK (DX5$^-$NK1.1$^+$) and mNK cells (DX5$^+$ NK1.1$^+$) and analyzed for *Tcf7*-GFP expression (open histograms) as compared cells from non-reporter mice (WT, gray fill).

(D and E) CD3$^-$NK1.1$^+$ spleen NK cells were subdivided into progressively mature NK cell populations (CD27$^+$CD11b$^-$ → CD27$^+$CD11b$^+$ → CD27$^-$CD11b$^+$) and analyzed for (D) *Tcf7*-GFP expression (open histograms) as compared cells from non-reporter mice (WT, gray fill) or (E) intracellular Tcf1 staining in *Tcf7*$^{+/+}$ (open histograms) as compared to *Tcf7*$^{-/-}$ control NK cell populations (gray fill).

Data are representative of three to five independent experiments. See also Figure S1.

Tcf1 Deficiency Results in Excessive Granzyme Expression

To understand the role of Tcf1 for NK cell development, we determined the cellular basis for defective NK cell development in the absence of Tcf1. BM mNK cells go through a stage of active proliferation (Kim et al., 2002), which was not impaired in the absence of Tcf1 (Figure 4A). Rather, *Tcf7*$^{-/-}$ BM NK cells showed evidence of enhanced cell death (Figure 4B). Since NK cell development, homeostasis, and expansion chiefly depend on IL-15 signaling, we determined whether splenic NK cells from *Tcf7*$^{-/-}$ mice were responsive to IL-15 or IL-2 in vitro. Cytokine stimulation of *Tcf7*$^{-/-}$ NK cells induced normal activation, cell-cycle progression (Figure S4A), and as many cell divisions as observed in *Tcf7*$^{+/+}$ NK cells (Figure 4C). Notwithstanding, *Tcf7*$^{-/-}$ NK cells failed to accumulate in number (Figure 4D). This was accounted for by an increased abundance of apoptotic NK cells (Figures 4E and S4B). When *Tcf7*$^{+/+}$ and *Tcf7*$^{-/-}$ NK cells were mixed before stimulation, *Tcf7*$^{+/+}$ NK cells expanded efficiently, while *Tcf7*$^{-/-}$ NK cells did not (Figure 4F). Thus, the reduced expansion of *Tcf7*$^{-/-}$ NK cells in vitro was due to cell-autonomous apoptosis rather than reciprocal killing (fratricide).

To elucidate the basis for deficient NK cell development and expansion, we established the global gene expression profiles of flow-sorted BM mNK cells from *Tcf7*$^{+/+}$ and *Tcf7*$^{-/-}$ mice. Based on three independent datasets, 20 of 28,000

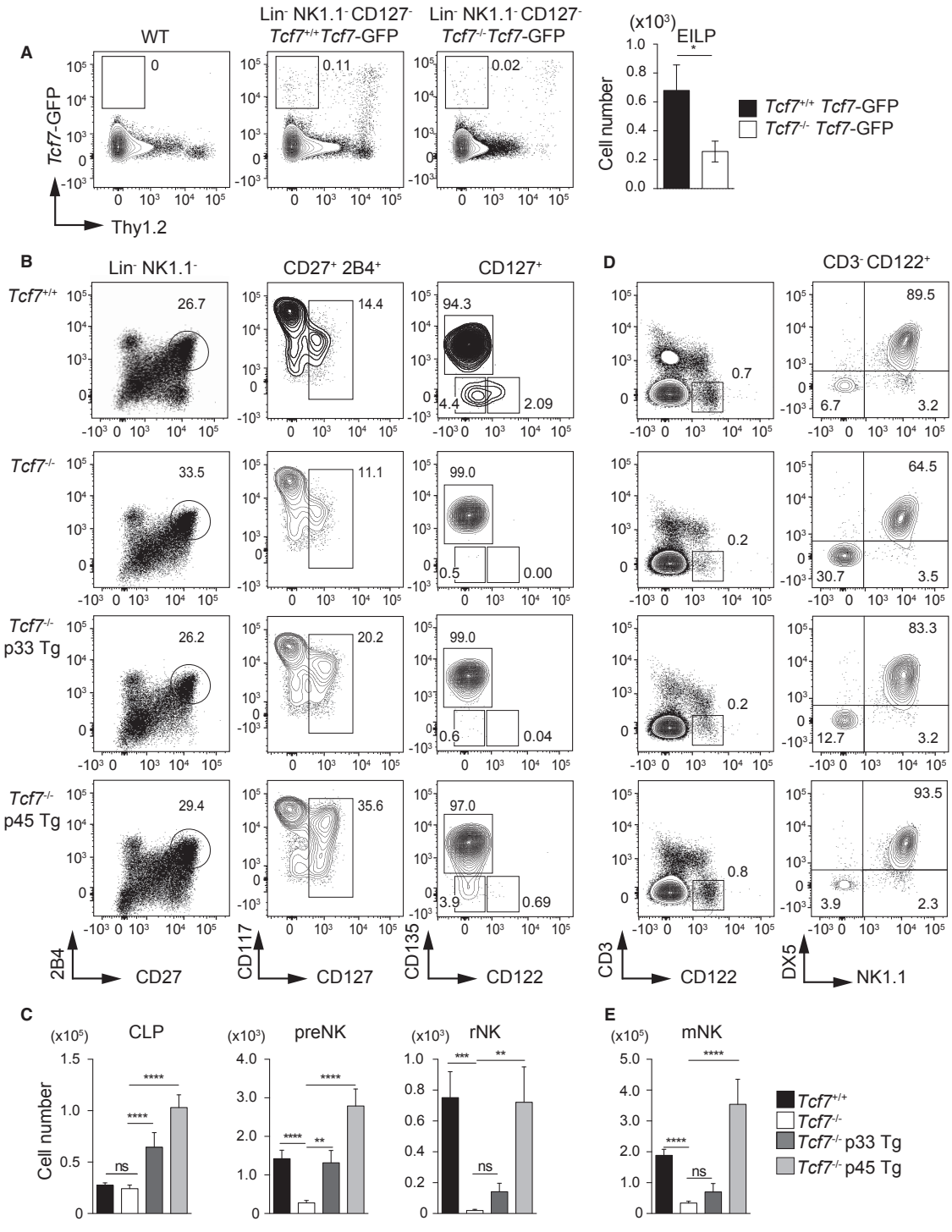

Figure 2. Tcf1-Dependent Stages of NK Cell Development

(A) Lin⁻NK1.1⁻CD127⁻ BM cells from *Tcf7*$^{+/+}$ *Tcf7*-GFP, *Tcf7*$^{-/-}$ *Tcf7*-GFP and from non-reporter (WT) mice analyzed for the presence of Thy1⁻ *Tcf7*-GFP⁺ cells. Numbers indicate the percentage of cells in the respective gate. Bar graph depicts the mean (±SEM) number of Lin⁻NK1.1⁻CD127⁻Thy1⁻ *Tcf7*-GFP⁺ (EILP) cells per femur from six or seven mice from three independent experiments.

(B–E) Flow cytometry analysis of BM from *Tcf7*$^{+/+}$, *Tcf7*$^{-/-}$, *Tcf7*$^{-/-}$ p33 Tg, and *Tcf7*$^{-/-}$ p45 Tg mice. (B) Lin⁻NK1.1⁻ BM cells were analyzed for 2B4 versus CD27 expression (left). Gated 2B4⁺ CD27⁺ cells were further analyzed for CD127 versus CD117 (middle), and gated CD127⁺ cells were analyzed for CD135 and CD122 to identify CLP (CD135⁺CD122⁻), pre-NK (CD135⁻CD122⁻), and rNK cells (CD135⁻CD122⁺). Numbers indicate the percentage of cells in the respective gate. (D) BM cells were analyzed for CD3 versus CD122 (left), and gated CD3⁻CD122⁺ NK cells were analyzed for the presence of mNK (DX5⁺NK1.1⁺) (right). Numbers

(legend continued on next page)

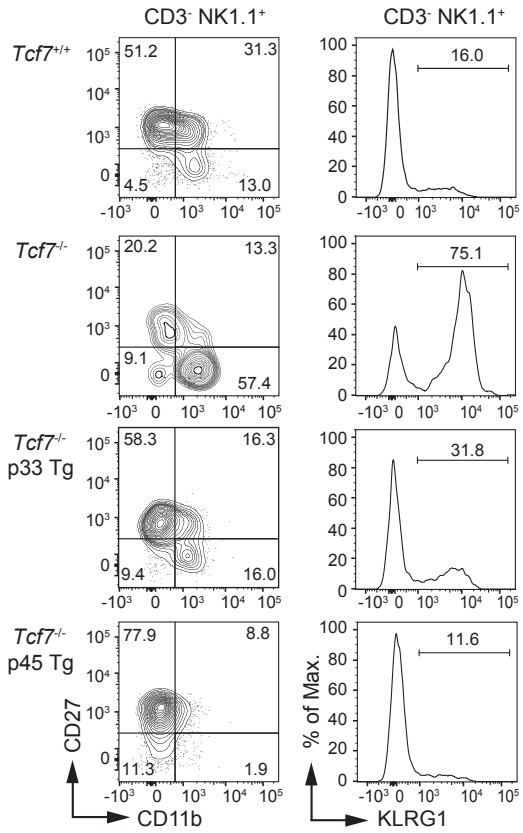

Figure 3. Absence of Tcf1 Increases and Enforced p45 Tcf1 Expression Counteracts Terminal NK Cell Maturation

Gated CD3⁻NK1.1⁺ BM NK cells from *Tcf7*$^{+/+}$, *Tcf7*$^{-/-}$, *Tcf7*$^{-/-}$ p33 Tg, and *Tcf7*$^{-/-}$ p45 Tg mice were analyzed for the expression of CD27 versus CD11b (left) or KLRG1 (right). Numbers indicate the percentage of cells in the corresponding gate. Data are representative of five independent experiments. See also Figure S3.

genes were differentially expressed (adjusted p value $p < 0.05$), whereby 15 genes were upregulated and 5 were downregulated in *Tcf7*$^{-/-}$ compared to *Tcf7*$^{+/+}$ BM mNK cells (Table S1). The search for differentially expressed genes that are associated with the Gene Ontology (GO) term "apoptosis" identified members of the granzyme family. *Gzmb* (2.5-fold, $p < 0.05$) and *Granzyme C* (*Gzmc*) (2.5-fold, $p < 0.05$) were upregulated in Tcf1-deficient mNK cells (Table S1). *Granzyme K* (*Gzmk*) and *Granzyme A* (*Gzma*) were also expressed at higher levels, even though the p values were >0.05 (data not shown). qRT-PCR analysis showed that *Gzmb* as well as *Gzma* and *Gzmk* were significantly overexpressed in *Tcf7*$^{-/-}$ BM mNK cells (Figure 5A), while *Gzmc* was below detection.

Granzymes are stored in lytic granules of NK cells and cytotoxic T cells, and their release triggers programmed cell death in target cells (Chowdhury and Lieberman, 2008). In addition to the induction of target cell death, leakage of GzmB from granules into the cytoplasm can also result in effector cell death (Ida et al., 2003; Zhang et al., 2006). For example, activated CD4^{+} T cells, which lack the intracellular GzmB inhibitor Spi6 (*Serpinb9*), undergo GzmB-mediated apoptosis (Zhang et al., 2006). We thus hypothesized that excessive granzyme expression, due to the absence of Tcf1, induced self-inflicted NK cell death.

To test this hypothesis, we analyzed GzmB protein expression in BM NK cells by intracellular flow cytometry. Even though wild-type BM mNK cells constitutively express *Gzmb* mRNA, GzmB protein expression is low (Figure 5B) (Fehniger et al., 2007). In contrast, GzmB was expressed at high levels in *Tcf7*$^{-/-}$ mNK cells (Figure 5B). This was not simply due to an increased abundance of terminally mature NK cells, which express higher levels of GzmB, as GzmB was globally increased also in immature (CD27^{+}CD11b^{-}) NK cells (Figure S4C). GzmB was also overexpressed in *Tcf7*$^{-/-}$ NK cells developing in mixed BM chimeras (Figure S4D), indicating that GzmB overexpression was not solely due to homeostatic effects. On the other hand, the expression of the GzmB inhibitor Spi6 (*Serpinb9*) was not different between *Tcf7*$^{+/+}$ and *Tcf7*$^{-/-}$ NK cells (Figure 5C). Thus, Spi6 levels in *Tcf7*$^{-/-}$ NK cells may be too low to neutralize GzmB leaking into the cytoplasm and prevent NK cell self-destruction.

To further address this possibility, we determined the intracellular localization of GzmB relative to the granule component Lamp1 (CD107a) using confocal microscopy. Cytokine stimulated wild-type NK cells contained several Lamp1^{+} granules per cross section, and GzmB co-localized with these Lamp1^{+} granules (Figure 5D, top). BM mNK cells from wild-type mice either lacked Lamp1^{+} granules (50%) or had very few Lamp1^{+} granules per cross section. These granules did not contain GzmB (Figures 5D and 5E, middle). Lamp1 expression was detected in 30% of *Tcf7*$^{-/-}$ BM mNK cells whereby Lamp1 expression was often diffuse (Figures 5D and 5E, bottom). Interestingly, a large fraction of *Tcf7*$^{-/-}$ mNK cells expressed GzmB, but not Lamp1. In such NK cells, GzmB frequently showed a diffuse cytoplasmic and occasionally nuclear localization (Figures 5D and 5E). The latter is a feature associated with the execution phase of GzmB-mediated apoptosis (Trapani et al., 1998). These data show that Tcf1 deficiency results in excessive expression and mislocalization of GzmB and suggest that these NK cells undergo GzmB-mediated self-killing.

Excessive Granzyme Expression Impairs NK Cell Development

We further addressed whether granzyme expression correlated with impaired NK cell development. In wild-type mice, *Gzmb*, *Gzma*, and *Gzmk* are not expressed at the pre-NK stage but are upregulated at the rNK stage (Figure 5F), which coincides with the acquisition of CD122. In the absence of Tcf1, *Gzmb*, *Gzma*, and *Gzmk* were super-induced at the rNK stage but

indicate the percentage of cells in the respective gate or quadrant. Bar graphs (C and E) depict the mean (±SEM) number of cells in the indicated population in *Tcf7*$^{+/+}$ (black), *Tcf7*$^{-/-}$ (open), *Tcf7*$^{-/-}$ p33 Tg (dark gray), and *Tcf7*$^{-/-}$ p45 Tg (light gray) mice. Data were compiled from 8 to 25 mice from at least six independent experiments.

Statistical significance was determined by one-way ANOVA but is only shown for selected comparisons (C and E) or by two-tailed Student's t test (A), where *$p < 0.05$, **$p < 0.01$, ***$p < 0.001$, ****$p < 0.0001$ and ns, not significant ($p > 0.05$). See also Figure S2.

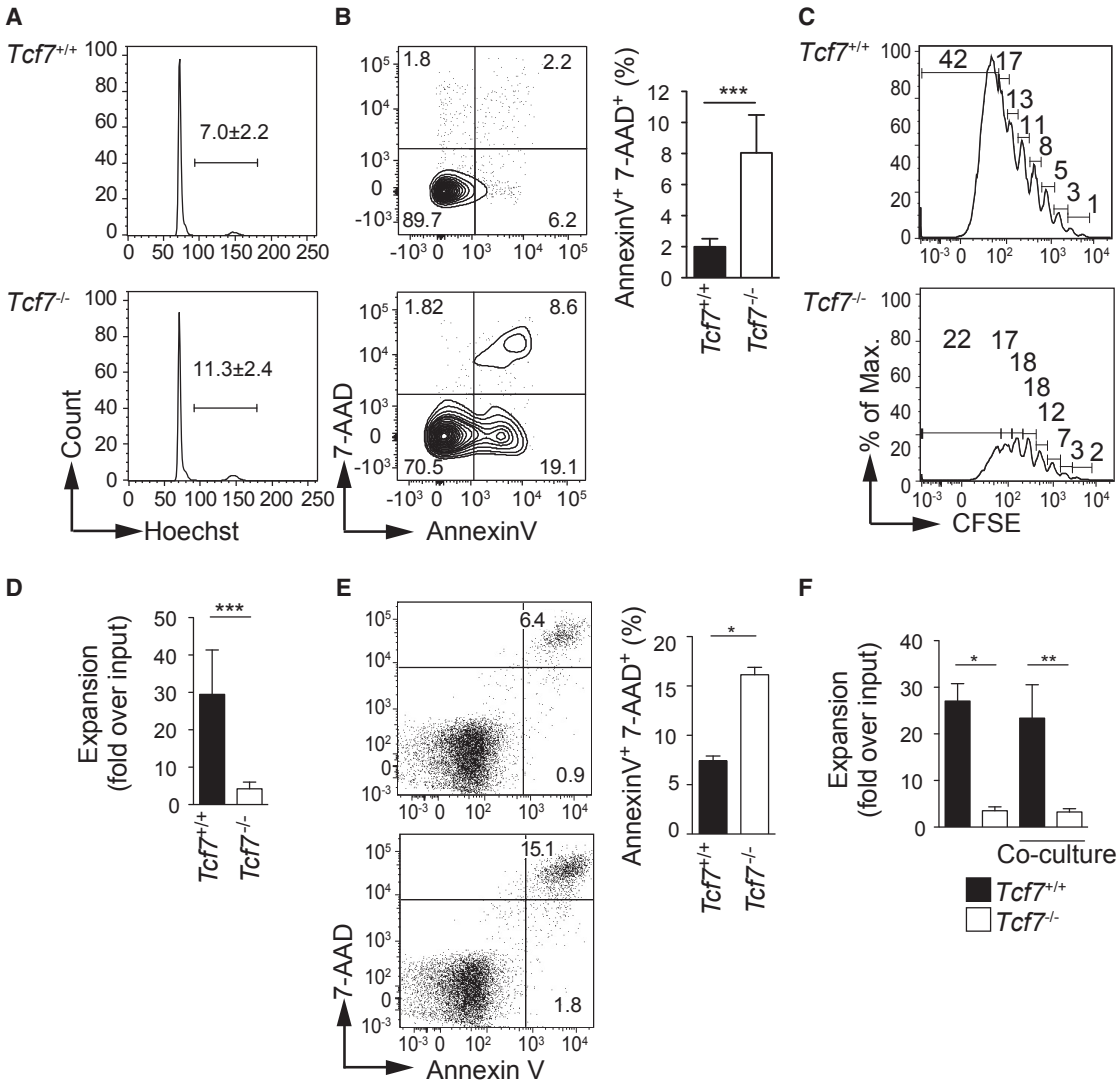

Figure 4. Tcf1 Ensures NK Cell Survival

(A) BM NK cells were stained with Hoechst to analyze DNA content. Numbers indicate the mean percentage (±SD) of Hoechst$^+$ *Tcf7*$^{+/+}$ and *Tcf7*$^{-/-}$ NK cells in the S, G2, or M phase of the cell cycle.

(B) Density plots show gated NK cells that had been incubated for 4 hr (in the absence of growth factor) at 37°C and then stained for Annexin V and 7-AAD. Bar graph depicts the mean percentage (±SD) of Annexin V$^+$ 7-AAD$^+$ NK cells from *Tcf7*$^{+/+}$ (black) and *Tcf7*$^{-/-}$ (open) mice.

Data in (A) and (B) are from two or more independent experiments and a total of three to six determinations.

(C) NK cell-enriched splenocytes were labeled with CFSE and cultured in IL-2. Histograms show the CFSE profile after 5 days of culture, and numbers indicate the percentage of cells in the corresponding gate.

(D) Bar graph depicts the mean fold expansion (±SD) of *Tcf7*$^{+/+}$ (black) and *Tcf7*$^{-/-}$ (open) NK cells at day 5 of IL-2 culture relative to input. Data are compiled from eight independent experiments.

(E) At day 5 of culture in IL-2, NK cells were stained with Annexin V and 7-AAD. Bar graph depicts the mean percentage (±SEM) of Annexin V$^+$ 7-AAD$^+$ NK cells from *Tcf7*$^{+/+}$ (black) and *Tcf7*$^{-/-}$ (open) mice. Data were compiled from two independent experiments.

(F) Purified NK cells from *Tcf7*$^{+/+}$ (CD45.1) and *Tcf7*$^{-/-}$ mice (CD45.2) were cultured separately or co-cultured at a 1:1 ratio, and NK cell numbers were determined on day 5 of culture in IL-2. Bar graphs depict the mean fold expansion (±SD) of *Tcf7*$^{+/+}$ (black) and *Tcf7*$^{-/-}$ NK cells (open) relative to input. Data are from three independent experiments.

Statistical significance was determined by two-tailed Student's t test (B and D–F), where *$p < 0.05$, **$p < 0.01$, and ***$p < 0.001$. See also Figure S4.

were not expressed prior to the rNK cell stage (Figure 5F). Thus, the acquisition of IL-15 responsiveness coincided with the induction of granzyme gene expression, which was limited by Tcf1. As NK cell development was restored in p45, but not in p33, Tg mice (Figures 2B–2E), we next analyzed granzyme expression in Tcf1 Tg BM NK cells. GzmB protein and mRNA levels were low in *Tcf7*$^{+/+}$ mNK cells, high in *Tcf7*$^{-/-}$ and *Tcf7*$^{-/-}$ p33 mNK cells, and low again in *Tcf7*$^{-/-}$ p45 mNK

cells (Figures 5G, 5H, and S4C). Corresponding expression patterns were observed for *Gzma* and *Gzmk* mRNA (Figure S4E). We concluded that the p45 Tg suppressed granzymes and that this was associated with the restoration of NK cell development.

We next asked whether granzyme deficiency rescued the developmental defect of *Tcf7*$^{-/-}$ NK cells. To address this, we crossed *Tcf7*$^{-/-}$ to *Gzmb*-cluster-deficient mice (*Gzmb*^{tm1Ley}) (Heusel et al., 1994), which lack *Gzmb* and have reduced *Gzmc*, *Gzmd*, and *Gzmf* expression (Revell et al., 2005). However, *Gzmb* cluster deficiency did not restore NK cell development in *Tcf7*$^{-/-}$ mice (Figure S5). As *Tcf7*$^{-/-}$ mice lacked pre-NK cells and granzymes were upregulated only at the rNK stage, we introduced the p33 Tg, which restores pre-NK cells. However, BM rNK and mNK cell development was still impaired in *Tcf7*$^{-/-}$ p33 Tg *Gzmb*$^{-/-}$ mice (Figure S5). *Tcf7*$^{-/-}$ NK cells also overexpressed *Gzma* and *Gzmk* (Figures 5A and 5F), which are in a separate gene cluster and may redundantly impair NK cell survival. To test whether granzyme overexpression impaired NK cell development, we transduced wild-type Lin^{-}NK1.1^{-} BM progenitor cells with retroviral constructs coding for granzymes, followed by in vitro differentiation toward the NK cell lineage with IL-15 (Williams et al., 1999). Compared to control transduction, enforced expression of *Gzmb* greatly reduced the differentiation of progenitors into NK cells, while there was no effect on B cells (Figure 5I). Enforced expression of *Gzma* or *Gzmk* similarly reduced NK cell differentiation in vitro (Figure S4F). These effects were NK cell intrinsic, since non-transduced NK cells present in the same cultures developed normally (Figure S4F). Thus, excessive expression of granzymes impaired NK cell development.

Increased GzmB Expression Impairs NK Cell-Mediated Target Cell Killing

We next addressed whether increased granzyme expression altered the ability of NK cells to kill target cells. To circumvent confounding effects due to a difference in NK cell maturation, we used cells from poly(I:C)-primed mice. We found that the lysis of MHC-I^{low} RMA/S tumor cells by poly(I:C)-primed *Tcf7*$^{-/-}$ NK cells was reduced 5- to 10-fold compared to wild-type NK cells (Figures 6A and 6B). In addition, *Tcf7*$^{-/-}$ NK cells also showed significantly reduced killing of YAC-1 cells (in part mediated by NKG2D), RMA cells transfected with m157 cells (Ly49H), and anti-Thy1 (CD90.2)-coated RMA cells (antibody-dependent cell-mediated cytotoxicity [ADCC]) (Figure 6B). RMA cells transfected with H60 (NKG2D) were killed equally efficiently by the two types of NK cells (Figure 6B). In addition, *Tcf7*$^{-/-}$ mice were severely impaired in their ability to reject MHC class I (β2 m)-deficient splenocytes in vivo (Figure 6C) and to prevent the outgrowth of primary B cell acute lymphoblastic leukemia (B-ALL) cells lacking β2 m (Figure 6D). The functional impairment was specific for target cell lysis, as *Tcf7*$^{-/-}$ NK cells efficiently released Lamp1 (CD107) when stimulated with various tumor target cells or with antibodies to specific activation receptors (Figures S6A and S6D). Moreover, activated *Tcf7*$^{-/-}$ NK cells had a normal ability to produce chemokines and cytokines (Figures S6A–S6C). Thus, NK cells from *Tcf7*$^{-/-}$ mice are educated and recognize target cells but have a severely reduced capacity to kill them.

Based on the increased death of cytokine-activated NK cells lacking Tcf1 (Figure 4E), we hypothesized that reduced target cell killing was due to the induction of NK cell death following activation by target cells. Indeed, *Tcf7*$^{-/-}$, but not *Tcf7*$^{+/+}$, NK cells underwent significant cell death when exposed to susceptible target cells (RMA/S), while resistant target cells (RMA) did not increase NK cell death (Figures 6E and 6F). To determine the basis for target-induced NK cell death, we exposed *Tcf7*$^{-/-}$ NK cells to susceptible RMA/S tumor cells in the presence of selected peptide-based inhibitors. The GzmB inhibitor (z-AAD-CMK) reduced target-induced apoptosis of *Tcf7*$^{-/-}$ NK cells, while a negative control peptide (z-FA-CMK) had no effect (Figures 6E and 6F). GzmB is activated by cathepsin-C-mediated cleavage of pro-GzmB. A cathepsin C inhibitor (DPPI) also reduced target-induced apoptosis of *Tcf7*$^{-/-}$ NK cells, while the control caspase inhibitor z-VAD had no effect (Figure 6F). Finally, *Gzmb* cluster deficiency also significantly reduced target-induced apoptosis of *Tcf7*$^{-/-}$ NK cells (Figure 6G). Thus, the reduced lytic activity of *Tcf7*$^{-/-}$ NK cells was accounted for by target-induced, GzmB-dependent death of *Tcf7*$^{-/-}$ NK cells.

Tcf1 Binding to a Regulatory Element Upstream of the *Gzmb* Locus Dampens *Gzmb* Expression

Given the importance of Tcf1-mediated repression of GzmB for NK cell development and function, we asked if *Gzmb* was a Tcf1 target gene. We prepared chromatin from IL-2-expanded NK cells to determine genome-wide Tcf1 binding using chromatin immunoprecipitation (ChIP) followed by deep sequencing (ChIP-seq). Tcf1 binding was further correlated with histone 3 lysine 4 tri-methylation (H3K4me3) deposition, which is an epigenetic mark of active chromatin.

We identified 751 Tcf1-binding peaks in *Tcf7*$^{+/+}$ relative to *Tcf7*$^{-/-}$ NK cells. We next addressed whether Tcf1 was associated with any of the 20 genes that are differentially expressed in *Tcf7*$^{+/+}$ relative to *Tcf7*$^{-/-}$ NK cells (Table S1). Considering ±50 kb flanking sequence, we noted Tcf1 binding to the *Tcf7* and *Gzmb* loci. A single Tcf1-binding element (TBE) was present ~26 kb upstream of the *Gzmb* transcriptional start site (Figure 7A), which was confirmed by ChIP-qPCR (Figure 7B). Tcf1 binding to the *Gzmb* TBE correlated with a reduction of activating H3K4me3 marks at the *Gzmb* gene locus (Figures 7A and 7C) and with reduced *Gzmb* expression (Figure 7D). Conversely, Tcf1 binding to the known target *Axin2* correlated with an increase of H3K4me3 marks (Figures S7A and S7C) and increased *Axin2* mRNA expression (Figure S7D). Thus, Tcf1 binding is associated with target gene activation or suppression.

To further define the function of the *Gzmb* TBE, we performed ChIP using antibodies against histone 3 lysine 4 mono-methylation (H3K4me1) and histone 3 lysine 27 acetylation (H3K27Ac), which are epigenetic marks associated with enhancer elements. In wild-type NK cells, the *Gzmb* TBE was associated with H3K4me1 and H3K27Ac marks (Figure 7E), indicating that the TBE is part of a *Gzmb* enhancer element. Interestingly, H3K4me1 and H3K27Ac marks at the TBE were significantly more abundant in *Tcf7*$^{-/-}$ NK cells (Figure 7E). These data suggested that Tcf1 binding reduced the function of a *Gzmb*-associated enhancer element. To further address this possibility, we cloned a 500-bp fragment, which comprised the *Gzmb* TBE

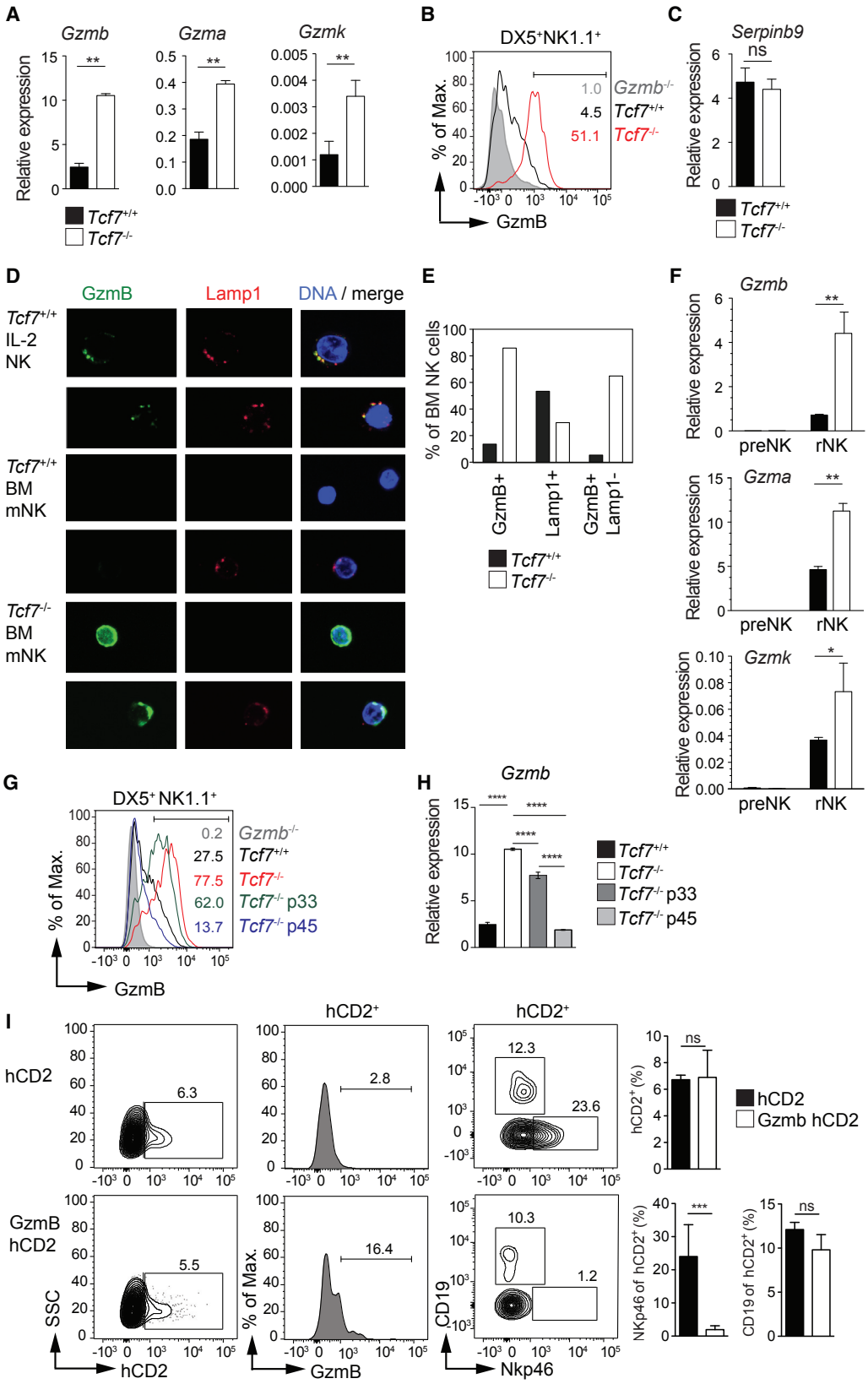

(legend on next page)

(Figure S7E), upstream of a minimal promoter and a luciferase reporter gene. We found that this element significantly enhanced reporter activity upon transient transfection into a GzmB-expressing cell line and that co-transfecting Tcf1 cDNA completely abrogated the increase (Figure 7F). Thus, Tcf1 binding reduced the activity of a Gzmb-associated enhancer element, which accounted for the reduced *Gzmb* expression in Tcf1-expressing NK cells.

DISCUSSION

The transcription factor Tcf1 is essential for the development of NK cells, but its precise role has not been completely understood. Based on the analysis of Tcf1-deficient and Tcf1-transgenic mice, we propose that Tcf1 guides NK cells through three stages of development and maturation. Tcf1 expression directed BM progenitors toward the NK cell lineage and ensured the survival of NK-committed cells, and its downregulation was essential for terminal NK cell maturation. In NK-lineage-committed cells, Tcf1 suppressed GzmB and additional granzyme family members, and this prevented NK cell self-destruction during development. Tcf1 also protected mature NK cells from GzmB-dependent self-destruction upon activation with cytokines or susceptible target cells. Thus, negative regulation of granzyme expression by Tcf1 played an essential role for the normal expansion and function of NK-committed cells. Protection from self-destruction was a stage-specific role of Tcf1, since pre-NK cells, which also depended on Tcf1, did not express granzymes.

Unexpectedly, our transcriptome analysis of BM mNK cells did not identify transcription factors implicated in NK cell development as potential Tcf1 targets. This was confirmed using qRT-PCR analyses, which indicated only minor expression changes of *Nfil3*, *Id2*, and *Tbx21* (T-bet) in rNK cells lacking Tcf1. A more notable reduction was observed for *Eomes* (2-fold) (data not shown). However, *Eomes* deficiency does not grossly alter the size of the BM NK cell compartment (Gordon et al., 2012). On the other hand, granzyme expression can be detrimental, and cells need to protect themselves from the cell-intrinsic action of granzymes. Deletion of the intracellular GzmB inhibitor Spi-6 disrupted the integrity of lytic granules and resulted in accelerated GzmB-mediated death of activated $CD4^+$ T cells (Zhang et al., 2006). The observations suggested that GzmB leaks into the cytoplasm and that a cytoplasmic excess of GzmB relative to Spi6 results in self-destruction. Absence of Tcf1 in NK cells did not impact Spi6 expression, indicating that excessive GzmB expression overcame the protective effect of Spi6. Self-destruction via GzmB leakage is not restricted to mutant NK cells, as this was also shown when wild-type NK cells were activated with monoclonal antibodies (mAbs) to certain activation receptors (Ida et al., 2003). Interestingly, GzmB-mediated self-destruction is not restricted to cytotoxic effector cells, as it is also observed in hematopoietic stem cells (HSCs) lacking *c-myc* and *N-myc* or when wild-type HSCs are exposed to an inflammatory environment or chemotherapy (Carnevalli et al., 2014). It will thus be of interest to determine whether different cell types use similar mechanisms to limit GzmB expression.

Our mechanistic analyses suggested that Tcf1 binding reduced the activity of a *Gzmb*-associated regulatory element, and that could account for the reduced *Gzmb* expression in Tcf1-expressing NK cells. Based on the original targeting of the *Gzmb* gene (Pham et al., 1996; Revell et al., 2005), it was proposed that the expression of *Gzmb* and linked genes is coordinated by a locus control region (LCR) region. As we identified a single TBE associated with the *Gzmb* cluster, yet several Gzm genes were increased in the absence of Tcf1, it is tempting to speculate that the regulatory element identified herein represents the putative LCR. However, further work will be needed to verify this hypothesis. On the other hand, *Gzma* and *Gzmk*, which reside in a separate gene cluster, were also

Figure 5. Tcf1 Deficiency Results in Excessive Granzyme Expression and Mislocalization

(A) qRT-PCR analysis of flow-sorted BM mNK cells from $Tcf7^{+/+}$ (black) and $Tcf7^{-/-}$ (open) mice for *Gzmb, Gzma*, and *Gzmk*. Data are representative of three independent experiments. Error bars are SEM.

(B) Histogram overlay shows granzyme B (GzmB) expression in gated BM mNK cells from $Tcf7^{+/+}$ (black) and $Tcf7^{-/-}$ mice (red) as compared to $Gzmb^{-/-}$ controls (gray fill).

(C) qRT-PCR analysis of BM mNK cells from $Tcf7^{+/+}$ (black) and $Tcf7^{-/-}$ (open) mice for *Serpin9b* (Spi6). Data are representative of three independent experiments. Error bars are SEM.

(D and E) Confocal microscopy of cytokine-stimulated NK cells from $Tcf7^{+/+}$ mice (top two panels) or BM mNK cells from $Tcf7^{+/+}$ mice (middle two panels) or from $Tcf7^{-/-}$ mice (bottom two panels) for GzmB (green), Lamp1 (red), and DNA/DAPI (blue). Colocalization of GzmB (green) and Lamp1 (red) in the merged images (right) is shown in yellow. (E) Bar graph shows the percentage of BM mNK cells from $Tcf7^{+/+}$ (black) and $Tcf7^{-/-}$ (open) mice that are $GzmB^+$ or $Lamp1^+$ or that express GzmB in the absence of Lamp1. Data are based on the analysis of cross sections from 70 cells per genotype.

(F) qRT-PCR analysis of pre-NK and rNK cells from $Tcf7^{+/+}$ (black) and $Tcf7^{-/-}$ (open) mice for *Gzmb*, *Gzma*, and *Gzmk*. Data are representative of two independent experiments. Error bars are SEM.

(G) Histogram overlay shows GzmB expression in gated BM mNK cells from $Tcf7^{+/+}$ (black), $Tcf7^{-/-}$ (red), $Tcf7^{-/-}$ p33 Tg (green), and $Tcf7^{-/-}$ p45 Tg mice (blue) compared to $Gzmb^{-/-}$ mice (gray fill).

(H) qRT-PCR analysis of BM mNK cells from $Tcf7^{+/+}$ (black), $Tcf7^{-/-}$ (open), $Tcf7^{-/-}$ p33 Tg (dark gray), and $Tcf7^{-/-}$ p45 Tg (light gray) mice for *Gzmb*. Data are representative of two or three independent experiments. Error bars are SEM.

(I) Lineage-negative (Lin^-) $NK1.1^-$ wild-type BM progenitors were transduced with a control retrovirus (expressing hCD2) or a retrovirus coding for GzmB followed by hCD2. Progenitors were then differentiated toward the NK cell lineage for 3–5 days using IL-15. Representative flow cytometry plots show the transduction efficiency ($hCD2^+$) (left), GzmB expression by gated $hCD2^+$ cells (middle), and NKp46 versus CD19 expression among $hCD2^+$ cells (right). Bar graphs depict the mean percentages (±SD) of transduced cells ($hCD2^+$) and of transduced cells expressing NKp46 (NK cells) or CD19 (B cells). Data were compiled from two independent experiments with a total of three to six determinations.

Statistical significance was determined by one-way ANOVA and is only shown for selected comparisons (H) or by two-tailed Student's t test (A, C, F, and I), where $^*p < 0.05$, $^{**}p < 0.01$, $^{***}p < 0.001$ and $^{****}p < 0.0001$ and ns, not significant $p > 0.05$. See also Figures S4 and S5.

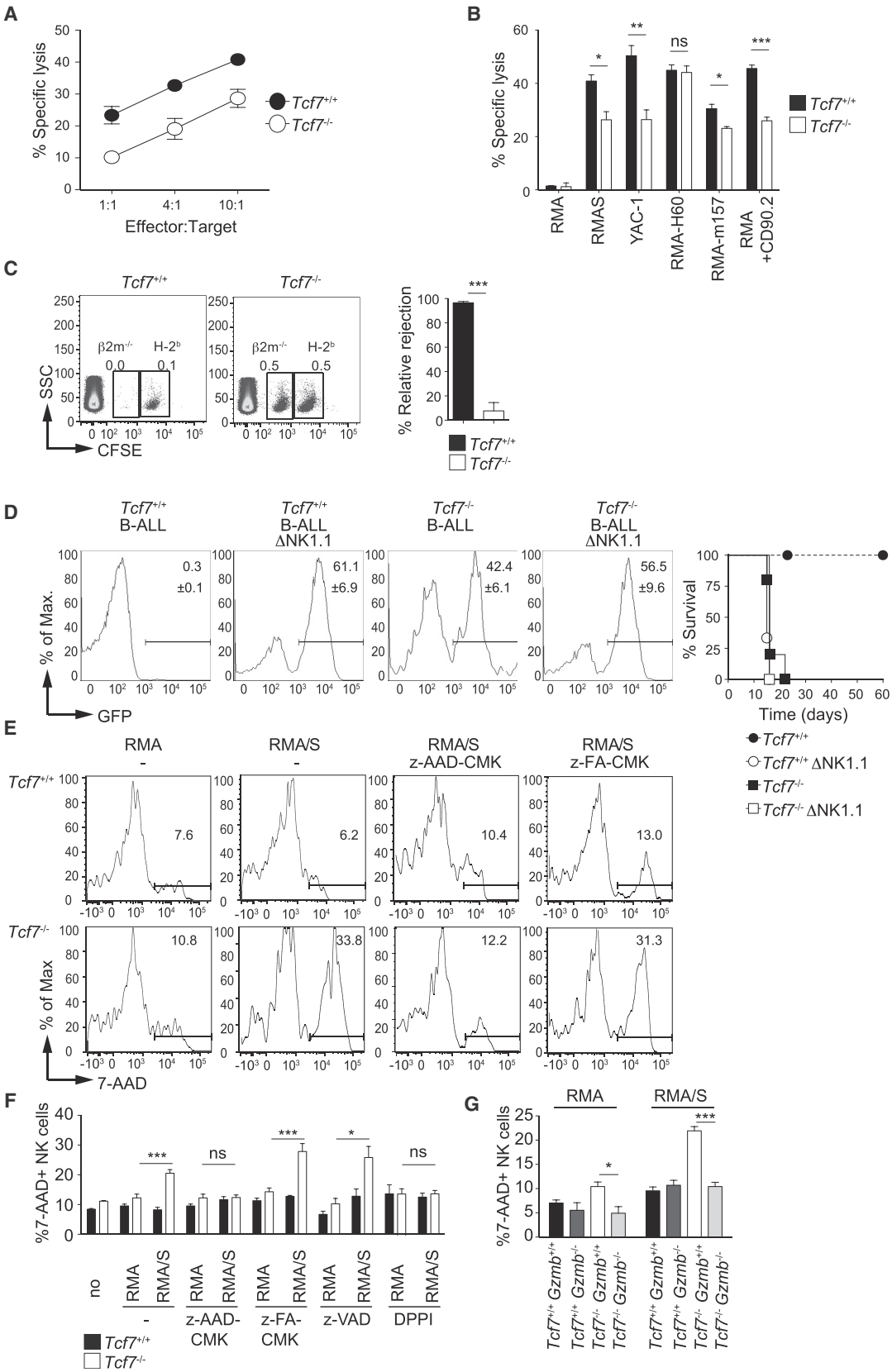

(legend on next page)

overexpressed in the absence of Tcf1, but we did not detect Tcf1 binding in the vicinity of the *Gzma* cluster. However, there is evidence for Tcf1 binding ~50 kb downstream of the *Gzma* cluster in $CD8^+$ thymocytes (Xing et al., 2016). In these cells, Tcf1 is also associated with *Gzmb*-associated regulatory element described herein. Thus, all granzymes may be subject to direct negative regulation by Tcf1.

Consistent with a negative regulatory role, Tcf1 can associate with Groucho/TLE co-repressors (Roose et al., 1998), exert histone deacetylase activity (Xing et al., 2016), or silence genes in cooperation with Runx3 (Steinke et al., 2014). These negative regulatory roles can be mediated by p33 and p45 Tcf1. However, p45, but not p33, suppressed *Gzmb* in NK cells. Tcf1 p45 can associate with β-catenin and/or γ-catenin, which usually promotes the expression of target genes, such as *Axin2*. However, there are few examples of target genes that are repressed by Tcf/β-catenin signaling, such as E-cadherin expression in the skin (Jamora et al., 2003). However, transcriptional repression by Tcf/β-catenin is poorly understood compared to transcriptional activation. Thus, the precise mechanism of Tcf1-mediated GzmB suppression will require further investigation. Irrespectively, we show that Tcf1 limits granzyme expression and that this is important to prevent NK cell self-destruction. Limiting the expression of granzymes thus represents an unexpected requirement for the proper development and function of NK cells.

EXPERIMENTAL PROCEDURES

Mice

C57BL/6 (B6) mice were purchased from Harlan OLAC. CD45.1 congenic B6 mice were bred in-house. $Tcf7^{-/-}$ (Verbeek et al., 1995), Tcf1 p33, and Tcf1 p45 transgenic (Ioannidis et al., 2001) and *Tcf7*-GFP reporter (Utzschneider et al., 2016), $Gzmb^{tm1Ley}$ *Gzmb*-cluster-deficient mice (termed $Gzmb^{-/-}$ herein) (Heusel et al., 1994) have been described previously. $Tcf7^{-/-}$ *Tcf7*-GFP, $Tcf7^{-/-}$ p33 Tg, $Tcf7^{-/-}$ p45 Tg, $Tcf7^{-/-}$ $Gzmb^{-/-}$, and $Tcf7^{-/-}$ p33 Tg $Gzmb^{-/-}$ mice were obtained by breeding. Animal experiments were performed in 6- to 12-week-old male or female mice in compliance with the University of Lausanne Institutional regulations and were approved by the veterinary authorities of the Canton de Vaud.

Flow Cytometry

Spleen and BM cells were treated with ACK buffer (0.15 M NH_4Cl, 1 mM $KHCO_3$, and 0.1 mM EDTA [pH 7.3]) to remove erythrocytes. Subsequently, cells were incubated with ZombieAqua (BioLegend) to exclude dead cells and anti-CD16/32 (2.4G2) hybridoma supernatant to block Fc receptors before staining with fluorescent mAbs (Table S2) for subsequent analyses or cell sorting using flow cytometry.

BM progenitor populations were identified by excluding cells stained for a cocktail of Alexa-Fluor-700-conjugated anti-CD3ε, CD4, CD8, CD11b, CD19, NK1.1, Ter119, and GR-1 mAbs. The resulting lineage-negative (Lin^-) cells were further labeled to identify CLP ($Lin^-2B4^+CD27^+CD127^+CD135^+CD122^-$), EILP ($Lin^-CD127^-Thy1^-$*Tcf7*-$GFP^+$), pre-NK ($Lin^-2B4^+CD27^+CD127^+CD135^-CD122^-$), rNK ($Lin^-2B4^+CD27^+CD127^+CD135^-CD122^+$), and mNK cells ($CD3^-CD122^+DX5^+NK1.1^+$). The maturation status of BM mNK and spleen NK cells was assessed using CD11b, CD27, and KLRG1 staining.

Intracellular staining for Tcf1 and GzmB was performed using the Foxp3 transcription factor staining buffer set (eBioscience) according to the manufacturer's protocol.

NK cell proliferation was assessed using Hoechst staining for ex vivo analyses or carboxyfluorescein succinimidyl ester (CFSE) dilution for NK cells cultured in vitro using recombinant human IL-2 (500 ng/mL) or IL-15. NK cell death was determined using 7-aminoactinomycin D (7-AAD) uptake with or without Annexin V staining.

Data were acquired on an LSRII or FACSCanto flow cytometer (Becton Dickinson) and analyzed with FlowJo (Tree Star). Alternatively, cells were subjected to sorting on a FACSAria (Becton Dickinson).

NK Cell Function and Target-Induced NK Cell Death

Mice were primed with 200 μg poly(I:C) (Labforce) intraperitoneally (i.p.), and spleens were harvested 24 hr later. Spleen cells were exposed to CFSE-labeled NK cell-resistant RMA ($H\text{-}2^b$) or susceptible RMA/S ($MHC\text{-}I^{low}$) cells. 4 hr later, 7-AAD was added, and the percentage of $7\text{-}AAD^+$ (dead) tumor cells among $CFSE^+$ target cells was determined by flow cytometry. Alternatively, 7-AAD uptake by gated NK cells ($CD3^-CD19^-NK1.1^+$) was used to assess target induced NK cell death in the absence or presence of the GzmB inhibitor (100 μM z-AAD-CMK), its negative control (100 μM z-FA-CMK) (Enzo), the

Figure 6. GzmB Mediates Target Cell-Induced NK Cell Death

(A) Splenocytes from poly(I:C) primed $Tcf7^{+/+}$ (black circles) or $Tcf7^{-/-}$ (open circles) mice containing equal numbers of NK cells were added to CFSE-labeled RMA/S ($MHC\text{-}I^{low}$) tumor cells at the indicated effector to target cell ratios. After 4–5 hr, 7-AAD uptake by tumor cells was used to determine target cell killing. The graph shows the mean percentage (±SD) of specific lysis of triplicate determinations at the indicated effector to target cell ratios. Data are representative of at least six independent experiments.

(B) Splenocytes from poly(I:C)-primed $Tcf7^{+/+}$ or $Tcf7^{-/-}$ mice containing equal numbers of NK cells were added to the indicated tumor target cells at a 10:1 effector/target ratio. Bar graph depicts the mean percentage (±SD) of specific tumor cell lysis ($7\text{-}AAD^+$) by $Tcf7^{+/+}$ (black) or $Tcf7^{-/-}$ (open) splenocytes from six independent experiments.

(C) B6 ($H\text{-}2^b$) and β2 $m^{-/-}$ splenocytes were labeled with a high and low dose of CFSE, respectively, before injection into $Tcf7^{+/+}$ or $Tcf7^{-/-}$ mice that had been primed with poly(I:C). The abundance of CFSE-labeled cells in the spleen was determined 24 hr later. Bar graph depicts the mean percentage (±SEM) rejection of β2 $m^{-/-}$ relative to $H\text{-}2^b$ splenocytes by $Tcf7^{+/+}$ *or* $Tcf7^{+/-}$ (black) or $Tcf7^{-/-}$ (open) mice. Data were compiled from three to five recipient mice from two independent experiments.

(D) BCR-ABL^+ (GFP^+) primary B cell acute leukemia (B-ALL) cell lines lacking β2 m were injected into $Tcf7^{+/+}$ (black circles) or $Tcf7^{-/-}$ (black squares) mice. Injection of anti-NK1.1 mAb into $Tcf7^{+/+}$ (open circles) or $Tcf7^{-/-}$ (open squares) mice was used to deplete NK cells (ΔNK1.1). Histograms depict the presence of B-ALL cells (GFP^+) in peripheral blood on day 10 after injection, and the graph depicts survival of mice over time. Similar data were obtained in a second experiment using poly(I:C)-primed mice.

(E and F) Splenocytes from poly(I:C)-treated $Tcf7^{+/+}$ and $Tcf7^{-/-}$ mice were exposed to NK cell-resistant RMA or NK cell-sensitive RMA/S tumor cells or cultured without tumor cells, in the absence of (–) or in the presence of a GzmB inhibitor (z-AAD-CMK), a negative control inhibitor (z-FA-CMK), a caspase inhibitor (z-VAD), or a cathepsin C inhibitor (DPPI). (E) Representative analysis of 7-AAD uptake by gated NK cells ($CD3^-CD19^-NK1.1^+$) after a 4 hr culture. (F) Bar graph depicts the mean percentage (±SEM) of $7\text{-}AAD^+$ NK cells from $Tcf7^{+/+}$ (black) and $Tcf7^{-/-}$ (open) mice. Data are from three to nine determinations.

(G) Splenocytes from poly(I:C)-treated $Tcf7^{+/+}$ $Gzmb^{+/+}$, $Tcf7^{+/+}$ $Gzmb^{-/-}$, $Tcf7^{-/-}$ $Gzmb^{+/+}$, and $Tcf7^{-/-}$ $Gzmb^{-/-}$ mice were exposed to RMA or RMA/S tumor cells. Bar graph depicts the mean percentage (±SEM) of $7AAD^+$ NK cells ($CD3^-CD19^-NK1.1^+$) 4 hr later. Data are from 3 to 11 determinations.

Statistical significance was determined by one-way ANOVA and is only shown for selected comparisons (G) or by Student's t test for the indicated comparisons (B, C, and F), where $^*p < 0.05$, $^{**}p < 0.01$, $^{***}p < 0.001$, and ns, not significant $p > 0.05$. See also Figure S6.

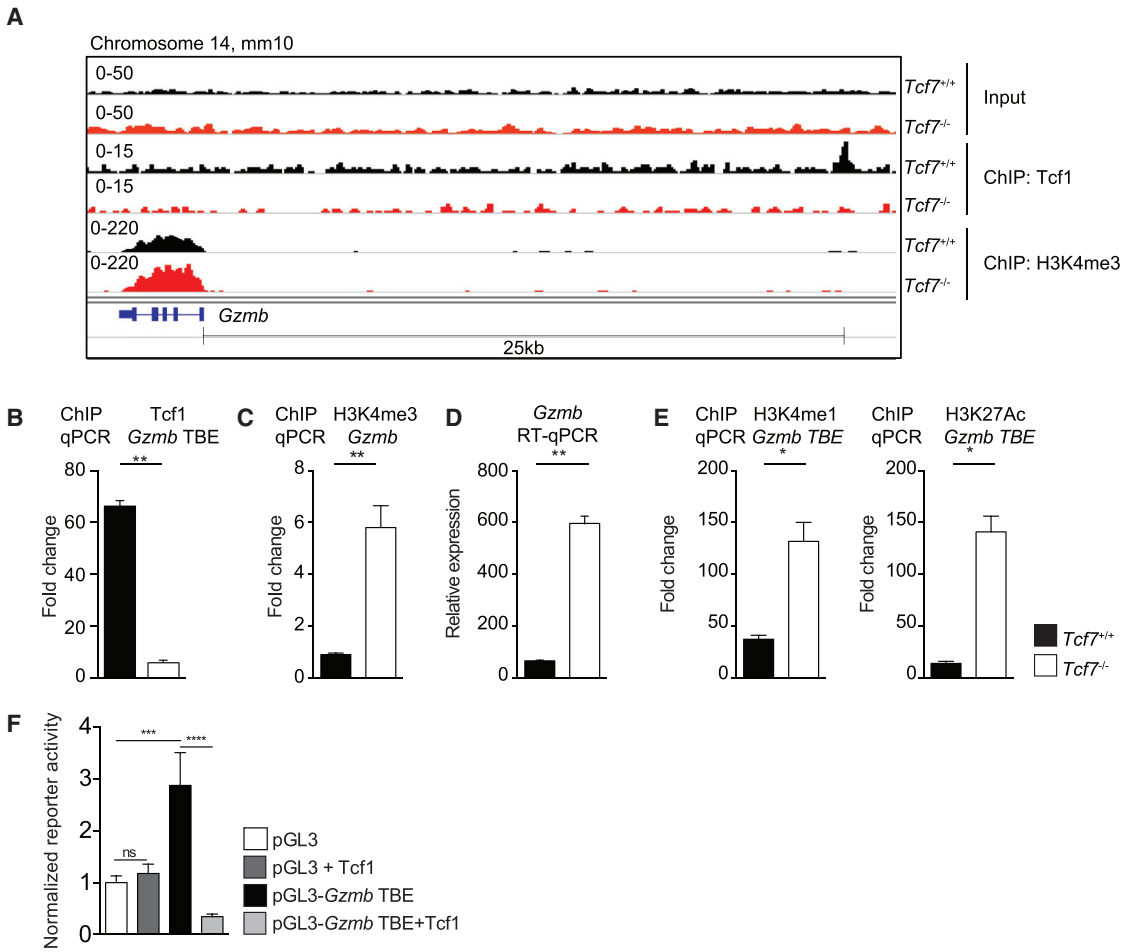

Figure 7. Tcf1 Binds to a Regulatory Element Upstream of the *GzmB* Locus

(A) Integrative genome viewer screenshots showing the ChIP-seq binding profiles of Tcf1, H3K4me3, and input (background) at the *GzmB* locus (+26 kb) in IL-2-activated NK cells isolated from *Tcf7*$^{+/+}$ (black tracks) and *Tcf7*$^{-/-}$ (red tracks) mice.

(B and C) IL-2-expanded NK cells from *Tcf7*$^{+/+}$ (black) and *Tcf7*$^{-/-}$ (open) mice were used for (B) Tcf1 or (C) H3K4me3 ChIP. qPCR was performed using primers surrounding the *GzmB* Tcf1-binding element (*Gzmb* TBE) (B) or the *Gzmb* gene (C). Results are expressed as fold change relative to control immunoglobulin G (IgG) ChIP. Data are representative of two or three experiments. Error bars are SEM.

(D) qRT-PCR analysis of *Gzmb* expression by IL-2-activated NK cells from *Tcf7*$^{+/+}$ (black) and *Tcf7*$^{-/-}$ (open) mice. Data are representative of two experiments. Error bars are SEM.

(E) IL-2-expanded NK cells from *Tcf7*$^{+/+}$ (black) and *Tcf7*$^{-/-}$ (open) mice were used for H3K4me1 and H3K27Ac ChIP followed by qPCR for the *Gzmb* TBE. Results are expressed as fold change relative to control IgG ChIP. Data are representative of two or three experiments. Error bars are SEM.

(F) Bar graph depicts reporter gene activity in transiently transfected CTLL-2 cells. Cells were transfected either with an empty pGL3 firefly luciferase vector (open) or a pGL3 vector containing a 500-bp fragment surrounding the *Gzmb* TBE (black), either without or with full-length Tcf1 (dark gray and light gray, respectively). Results were normalized to renilla luciferase transfection controls and subsequently to the results obtained with pGL3 alone. Data are compiled from three independent experiments. Error bars are SEM.

Statistical significance was determined by one-way ANOVA and is only shown for selected comparisons (F) or by two-tailed Student's t test (B–E), where *p < 0.05, **p < 0.01, ***p < 0.001, and ****p < 0.0001. See also Figure S7.

caspase inhibitor (50 μM z-VAD), or the cathepsin C inhibitor (15–25 μM DPPI) (MP Biomedicals).

Gene Expression and ChIP-Seq Analyses

Total cellular RNA from fluorescence-activated cell sorting (FACS)-purified *Tcf7*$^{+/+}$ and *Tcf7*$^{-/-}$ BM mNK cells was used for Affymetrix gene array analyses (GTF facility, University of Lausanne). Probe sets with adjusted p values (false discovery rate) <0.05 were used to identify differentially expressed genes.

For qPCR, cDNA was synthesized with oligo-dT or random hexamers, and PCR reactions were performed using the primers listed in Table S3 and a LightCycler FastStart DNA Master SYBR green I kit (Roche). Quantifications were done relative to *Hprt* using the LightCycler relative quantification software 1.0 (Roche).

For ChIP-seq, splenic NK cells were expanded in IL-2 for 5 days. 4 × 10^7 NK cells were cross-linked with 1% formaldehyde. Following lysis, chromatin was sheared to 0.3–1 kb before immunoprecipitation with antibodies specific for Tcf1, H3K4me3, H3K4me1, H3K27Ac, or a rabbit control antibody (Table S2) and protein-G agarose beads (Roche). Purified DNA was either used for qPCR with the primers indicated in Table S3 or sequenced. For sequencing, libraries were prepared using the NEBNext Chip-Seq Library Prep Master

Mix Set (NEB) and sequenced on a Illumina Hiseq 2500 (GTF facility, University of Lausanne). Reads were mapped to reference genome mm10/GRCm38 using Bowtie (version 2.1.0) and Peak calling was performed using MACS (version 1.4). Samples were compared using the UCSC genome browser or the Integrative Genome Browser.

Statistical Analysis

Statistical significance was determined using an unpaired two-tailed Student's t test for unequal variances or using a one-way ANOVA along with the Dunnett's post-test to adjust for multiple comparisons (using a 95% confidence interval). In all cases, p values are indicated as *$p < 0.05$, **$p < 0.01$, ***$p < 0.001$, ****$p < 0.0001$, and not significant (ns, $p > 0.05$).

Additional and more detailed experimental information is available in Supplemental Experimental Procedures.

ACCESSION NUMBERS

The accession number for the microarray and ChIP-seq data reported in this paper is GEO: GSE92711.

SUPPLEMENTAL INFORMATION

Supplemental Information includes Supplemental Experimental Procedures, seven figures, and one table and can be found with this article online at http://dx.doi.org/10.1016/j.celrep.2017.06.071.

AUTHOR CONTRIBUTIONS

B.J.-R. and J.G. designed and performed experimental work, analyzed the results, and prepared figures. M.C., V.C., and C.G. designed and performed experimental work and analyzed the results. P.A., B.J.-R., and M.D. analyzed the ChIP-seq data. W.H. conceived the study, supervised the project, and wrote the manuscript.

ACKNOWLEDGMENTS

We thank H. Clevers (Utrecht) for providing *Tcf7*$^{-/-}$ mice and C. Borner (Freiburg) for providing *Gzmb*-cluster-deficient mice. We are grateful to C. Fumey for mouse management, the UNIL Flow Cytometry Facility for assistance, and the UNIL Genomic Technology Facility for array and ChIP-seq analyses. This work was supported in part by grants from the Swiss National Science Foundation (SNSF) (310030B_141178 and 310030_159598 to W.H.) and funding by the Swiss government (State Secretariat for Education, Research and Innovation) of the SIB Swiss Institute of Bioinformatics for core service and infrastructure projects.

Received: January 20, 2017
Revised: May 19, 2017
Accepted: June 23, 2017
Published: July 18, 2017

REFERENCES

Carnevalli, L.S., Scognamiglio, R., Cabezas-Wallscheid, N., Rahmig, S., Laurenti, E., Masuda, K., Jöckel, L., Kuck, A., Sujer, S., Polykratis, A., et al. (2014). Improved HSC reconstitution and protection from inflammatory stress and chemotherapy in mice lacking granzyme B. J. Exp. Med. *211*, 769–779.

Carotta, S., Pang, S.H., Nutt, S.L., and Belz, G.T. (2011). Identification of the earliest NK-cell precursor in the mouse BM. Blood *117*, 5449–5452.

Chiossone, L., Chaix, J., Fuseri, N., Roth, C., Vivier, E., and Walzer, T. (2009). Maturation of mouse NK cells is a 4-stage developmental program. Blood *113*, 5488–5496.

Chowdhury, D., and Lieberman, J. (2008). Death by a thousand cuts: granzyme pathways of programmed cell death. Annu. Rev. Immunol. *26*, 389–420.

Delconte, R.B., Shi, W., Sathe, P., Ushiki, T., Seillet, C., Minnich, M., Kolesnik, T.B., Rankin, L.C., Mielke, L.A., Zhang, J.-G., et al. (2016). The helix-loop-helix protein ID2 governs NK cell fate by tuning their sensitivity to interleukin-15. Immunity *44*, 103–115.

Fathman, J.W., Bhattacharya, D., Inlay, M.A., Seita, J., Karsunky, H., and Weissman, I.L. (2011). Identification of the earliest natural killer cell-committed progenitor in murine bone marrow. Blood *118*, 5439–5447.

Fehniger, T.A., Cai, S.F., Cao, X., Bredemeyer, A.J., Presti, R.M., French, A.R., and Ley, T.J. (2007). Acquisition of murine NK cell cytotoxicity requires the translation of a pre-existing pool of granzyme B and perforin mRNAs. Immunity *26*, 798–811.

Gascoyne, D.M., Long, E., Veiga-Fernandes, H., de Boer, J., Williams, O., Seddon, B., Coles, M., Kioussis, D., and Brady, H.J. (2009). The basic leucine zipper transcription factor E4BP4 is essential for natural killer cell development. Nat. Immunol. *10*, 1118–1124.

Gordon, S.M., Chaix, J., Rupp, L.J., Wu, J., Madera, S., Sun, J.C., Lindsten, T., and Reiner, S.L. (2012). The transcription factors T-bet and Eomes control key checkpoints of natural killer cell maturation. Immunity *36*, 55–67.

Held, W., Kunz, B., Lowin-Kropf, B., van de Wetering, M., and Clevers, H. (1999). Clonal acquisition of the Ly49A NK cell receptor is dependent on the trans-acting factor TCF-1. Immunity *11*, 433–442.

Heusel, J.W., Wesselschmidt, R.L., Shresta, S., Russell, J.H., and Ley, T.J. (1994). Cytotoxic lymphocytes require granzyme B for the rapid induction of DNA fragmentation and apoptosis in allogeneic target cells. Cell *76*, 977–987.

Ida, H., Nakashima, T., Kedersha, N.L., Yamasaki, S., Huang, M., Izumi, Y., Miyashita, T., Origuchi, T., Kawakami, A., Migita, K., et al. (2003). Granzyme B leakage-induced cell death: a new type of activation-induced natural killer cell death. Eur. J. Immunol. *33*, 3284–3292.

Intlekofer, A.M., Takemoto, N., Wherry, E.J., Longworth, S.A., Northrup, J.T., Palanivel, V.R., Mullen, A.C., Gasink, C.R., Kaech, S.M., Miller, J.D., et al. (2005). Effector and memory CD8+ T cell fate coupled by T-bet and eomesodermin. Nat. Immunol. *6*, 1236–1244.

Ioannidis, V., Beermann, F., Clevers, H., and Held, W. (2001). The beta-catenin–TCF-1 pathway ensures CD4(+)CD8(+) thymocyte survival. Nat. Immunol. *2*, 691–697.

Jamora, C., DasGupta, R., Kocieniewski, P., and Fuchs, E. (2003). Links between signal transduction, transcription and adhesion in epithelial bud development. Nature *422*, 317–322.

Jeannet, G., Scheller, M., Scarpellino, L., Duboux, S., Gardiol, N., Back, J., Kuttler, F., Malanchi, I., Birchmeier, W., Leutz, A., et al. (2008). Long-term, multilineage hematopoiesis occurs in the combined absence of beta-catenin and gamma-catenin. Blood *111*, 142–149.

Kim, S., Iizuka, K., Kang, H.-S.P., Dokun, A., French, A.R., Greco, S., and Yokoyama, W.M. (2002). In vivo developmental stages in murine natural killer cell maturation. Nat. Immunol. *3*, 523–528.

Male, V., Nisoli, I., Kostrzewski, T., Allan, D.S., Carlyle, J.R., Lord, G.M., Wack, A., and Brady, H.J. (2014). The transcription factor E4bp4/Nfil3 controls commitment to the NK lineage and directly regulates Eomes and Id2 expression. J. Exp. Med. *211*, 635–642.

Molenaar, M., van de Wetering, M., Oosterwegel, M., Peterson-Maduro, J., Godsave, S., Korinek, V., Roose, J., Destrée, O., and Clevers, H. (1996). XTcf-3 transcription factor mediates beta-catenin-induced axis formation in Xenopus embryos. Cell *86*, 391–399.

Pham, C.T., MacIvor, D.M., Hug, B.A., Heusel, J.W., and Ley, T.J. (1996). Long-range disruption of gene expression by a selectable marker cassette. Proc. Natl. Acad. Sci. USA *93*, 13090–13095.

Revell, P.A., Grossman, W.J., Thomas, D.A., Cao, X., Behl, R., Ratner, J.A., Lu, Z.H., and Ley, T.J. (2005). Granzyme B and the downstream granzymes C and/or F are important for cytotoxic lymphocyte functions. J. Immunol. *174*, 2124–2131.

Robbins, S.H., Tessmer, M.S., Mikayama, T., and Brossay, L. (2004). Expansion and contraction of the NK cell compartment in response to murine cytomegalovirus infection. J. Immunol. *173*, 259–266.

Roose, J., Molenaar, M., Peterson, J., Hurenkamp, J., Brantjes, H., Moerer, P., van de Wetering, M., Destrée, O., and Clevers, H. (1998). The Xenopus Wnt

effector XTcf-3 interacts with Groucho-related transcriptional repressors. Nature *395*, 608–612.

Steinke, F.C., Yu, S., Zhou, X., He, B., Yang, W., Zhou, B., Kawamoto, H., Zhu, J., Tan, K., and Xue, H.H. (2014). TCF-1 and LEF-1 act upstream of Th-POK to promote the CD4(+) T cell fate and interact with Runx3 to silence Cd4 in CD8(+) T cells. Nat. Immunol. *15*, 646–656.

Stetson, D.B., Mohrs, M., Reinhardt, R.L., Baron, J.L., Wang, Z.-E., Gapin, L., Kronenberg, M., and Locksley, R.M. (2003). Constitutive cytokine mRNAs mark natural killer (NK) and NK T cells poised for rapid effector function. J. Exp. Med. *198*, 1069–1076.

Trapani, J.A., Jans, D.A., Jans, P.J., Smyth, M.J., Browne, K.A., and Sutton, V.R. (1998). Efficient nuclear targeting of granzyme B and the nuclear consequences of apoptosis induced by granzyme B and perforin are caspase-dependent, but cell death is caspase-independent. J. Biol. Chem. *273*, 27934–27938.

Utzschneider, D.T., Charmoy, M., Chennupati, V., Pousse, L., Ferreira, D.P., Calderon-Copete, S., Danilo, M., Alfei, F., Hofmann, M., Wieland, D., et al. (2016). T cell factor 1-expressing memory-like CD8(+) T cells sustain the immune response to chronic viral infections. Immunity *45*, 415–427.

Verbeek, S., Izon, D., Hofhuis, F., Robanus-Maandag, E., te Riele, H., van de Wetering, M., Oosterwegel, M., Wilson, A., MacDonald, H.R., and Clevers, H. (1995). An HMG-box-containing T-cell factor required for thymocyte differentiation. Nature *374*, 70–74.

Vosshenrich, C.A., Ranson, T., Samson, S.I., Corcuff, E., Colucci, F., Rosmaraki, E.E., and Di Santo, J.P. (2005). Roles for common cytokine receptor gamma-chain-dependent cytokines in the generation, differentiation, and maturation of NK cell precursors and peripheral NK cells in vivo. J. Immunol. *174*, 1213–1221.

Williams, N.S., Klem, J., Puzanov, I.J., Sivakumar, P.V., Bennett, M., and Kumar, V. (1999). Differentiation of NK1.1+, Ly49+ NK cells from flt3+ multipotent marrow progenitor cells. J. Immunol. *163*, 2648–2656.

Xing, S., Li, F., Zeng, Z., Zhao, Y., Yu, S., Shan, Q., Li, Y., Phillips, F.C., Maina, P.K., Qi, H.H., et al. (2016). Tcf1 and Lef1 transcription factors establish CD8(+) T cell identity through intrinsic HDAC activity. Nat. Immunol. *17*, 695–703.

Yang, Q., Li, F., Harly, C., Xing, S., Ye, L., Xia, X., Wang, H., Wang, X., Yu, S., Zhou, X., et al. (2015). TCF-1 upregulation identifies early innate lymphoid progenitors in the bone marrow. Nat. Immunol. *16*, 1044–1050.

Zhang, M., Park, S.M., Wang, Y., Shah, R., Liu, N., Murmann, A.E., Wang, C.R., Peter, M.E., and Ashton-Rickardt, P.G. (2006). Serine protease inhibitor 6 protects cytotoxic T cells from self-inflicted injury by ensuring the integrity of cytotoxic granules. Immunity *24*, 451–461.